의학박사 학위논문

Design and evaluation of a patient-specific 3D couplant pad for ultrasound image-guided radiation therapy

초음파영상유도방사선치료를 위한

환자 맞춤형 3차원 패드의 설계 및 평가

2016 년 2 월

서울대학교 대학원

의학과 의공학 전공

김 희 정

Design and evaluation of a patient-specific 3D couplant pad for ultrasound image-guided radiation therapy

지도 교수 최 진 욱

이 논문을 의학박사 학위논문으로 제출함
2015 년 10 월

서울대학교 대학원
의학과 의공학 전공
김 희 정

김희정의 의학박사 학위논문을 인준함
2015 년 12 월

위 원 장 김 일 한 (인)

부위원장 최 진 욱 (인)

위 원 김 희 찬 (인)

위 원 예 성 준 (인)

위 원 김 철 홍 (인)

Abstract

Design and evaluation of a patient-specific 3D couplant pad for ultrasound image-guided radiation therapy

Hee Jung Kim

Department of Biomedical Engineering

The Graduate School

Seoul National University

Purpose: Successful patient treatment with ultrasound image-guided radiation therapy (US IGRT) has been hindered by several issues, including patient deformation due to probe pressure, the presence of an image dead zone, and optical tracking disabilities caused by irregular surfaces. The purpose of this study was to overcome these barriers by using a patient-specific three-dimensional (3D) couplant pad created by a patient's skin mold using a 3D printing technique.

Materials and Methods: Commercial ultrasound-based localization systems (Clarity® 3.1; Elekta Ltd., Montréal, Québec, Canada) equipped with optical tracking devices were installed in a CT simulation room and in a radiation

treatment room. To determine the optimal materials for the couplant pad, various mixing ratios of candidate materials were used and the strengths and elasticities of the resultant couplant pads were tested. A patient skin mold was designed using a skin contour of simulation CT images and fabricated by a 3D printer (CubePro® , Cubify, 3DSYSTEMS, Rock Hill, SC, USA). A couplant pad was then fabricated by pouring gelatin solution into a fixed-shape container accommodating the patient's skin mold. To examine the effect of the couplant pad on the baseline positional accuracy of our system, a phantom study was carried out with a breast phantom. From the four patients who underwent US IGRT, a total of 486 ultrasound images (including images with and without the couplant pad) were acquired before treatment. The effectiveness of the couplant pad was evaluated in terms of image contrast, tracking accuracy, and inter-observer variation.

Results: The positioning accuracies of our US system in the phantom study were 0.9 ± 0.3 mm and 1.3 ± 0.4 mm with and without the couplant pad, respectively. The patient study revealed that if the US image acquired in the first radiation treatment session is used as a reference, the couplant pad can reduce the mean target shift from 4.7 mm to 3.7 mm in 3D vector amplitude. Moreover, the use of the couplant pad reduced the standard deviation from 2.2 mm to 1.7 mm. Use of the couplant pad also improved image contrast around the treatment target by 10 %. Analysis of the effect of US scanning coverage and target deformation due to excessive probe pressure revealed that the centroid offset of the target volume after target position alignment was decreased from 4.4 mm to 2.9 mm upon use of the couplant pad. Inter-fractional target contour agreement calculations revealed that one patient with a small target showed a substantial increase in the Kappa value (from 0.07 to 0.31) with the use of the couplant pad; however, this effect was not

significant in other cases with larger targets.

Conclusion: Our patient-specific 3D couplant pad, which was generated using a mold by 3D printing technique, is thus a promising strategy for improving tracking accuracy, image quality, and inter-observer variation for ultrasound-based image guided radiotherapy. In addition to its conventional advantage of noninvasiveness, our couplant pad facilitates the use of ultrasound technology in radiotherapy. Since the position, shape, and volume of the treatment target can be confirmed at every treatment, US is more effective for adaptive radiation therapy compared with conventional x-ray imaging.

Keywords: Ultrasound, Image-guided radiation therapy, 3D couplant, patient-specific pad

Student Number: 2009-31099

List of Tables

List of Figures

Table of Contents

1. Introduction

Cancer is a leading cause of death in Korea, with early diagnosis and proper treatment being crucial for achieving good outcomes.(1) Radiation treatment (RT) has been a main cancer treatment modality over the past several decades and is still evolving rapidly, thanks to new state-of-the-art technologies. Current efforts for improving RT focus on sparing more normal tissue, thus reducing side effects, and delivering more accurate doses to cancer cells, thereby enhancing the desired therapeutic effects.

To ensure optimal therapeutic effects and minimal side effects, two important concepts have been introduced to modern RT: (1) radiation treatment planning in conjunction with 3D volumetric imaging, and (2) image guided radiation treatment (IGRT) enabled by treatment room localization systems that provide 2D or 3D images of a patient during a treatment session.

A typical IGRT session consists of the following procedures: (1) determining the patient treatment setup position and the immobilization device; (2) acquiring simulation CT images for treatment planning; (3) establishing and verifying the treatment plan; (4) acquiring patient images in the treatment room to verify the patient position with respect to the planned position; and (5) repositioning the patient if the positioning error is beyond the acceptable criteria.

To date, a variety of imaging modalities have been introduced and used for IGRT. X-ray imaging has been the most popular solution for IGRT due to its cost-effectiveness and accuracy. In most RT facilities, X-ray images such as fluoroscopy,

2D radiography, and kV cone-beam CT images are widely used to verify patient setup prior to treatment. However, patient X-ray exposure is often regarded to be invasive and thus has had limited use.

Other IGRT solutions without x-rays include optical tracking systems, magnetic resonance imaging (MRI), electromagnetic transponder-based tracking, and ultrasound (US) systems. Even though MRI is well known for its noninvasiveness and superior soft tissue contrast, the optimal manner to integrate this technique into a medical linear accelerator (LINAC) is still being investigated due to the issue of electromagnetic interference. Optical tracking systems may be the most cost-effective IGRT solution due to their noninvasiveness. However, their use is severely limited to monitoring patient surfaces. Electromagnetic transponders may be convenient for monitoring internal organs in real time. However, the main drawback of this technique is that patients are required to undergo a one-time surgical procedure in which the transponders are placed near the treatment region.

Compared with these IGRT modalities, US has unique advantages. For instance, US can provide superior soft tissue contrast and high spatial resolution (i.e. in the sub-millimeter range).(2) Moreover, US is completely noninvasive, which potentially allows for frequent image guidance over the course of RT.

One of the most widely used US applications in RT is a B-mode acquisition and tracking system (BAT; Nomos, Cranberry Township, PA, USA), which was first introduced in the 1990s.(3) However, since US images were registered to simulation CT images in the BAT system, inter-modality discrepancy has been reported in several studies.(3-5)

The most up-to-date US imaging system for IGRT is Clarity® (Elekta Ltd., Montréal, Québec, Canada). The advantage of this system over the conventional

BAT system is that it eliminates inter-modality discrepancy by installing US devices in both a CT simulation room and a treatment room. The US images acquired from the CT simulation room can thus be used as reference images as patient treatments are set up.

To achieve optimal US image quality, all air gaps between the US probe and the patient's skin must be removed. For this reason, US scanning is performed by applying pressure to the probe, which can potentially deform the scanning region. As a result, target position discrepancies between the simulation and the treatment can occur, as well as image distortion.(4,6-9) Since pressure is applied manually to the US probe, its effects can vary depending on the operator. Thus, high inter-observer variation has been a major issue in US IGRT systems. Moreover, since US imaging involves the manual movement of a probe device over potentially irregular patient surfaces, inter-observer variation can be also an issue. Therefore, achieving consistent and reproducible US scanning requires adequate user experience and training.(7,8)

To minimize these problems, the American Association of Physicists in Medicine (AAPM) has recommended that operators use sufficient US coupling gel and minimum probe pressure. However, since an RT course consists of multiple fractions scheduled over 7-8 weeks, it is difficult for even a skilled operator to maintain scanning procedure consistency over the entire treatment period.(10)

For targets near the skin, a sufficient depth of US coupling gel is required to avoid image distortion.(11,12) However, typical US coupling gel products have relatively low viscosity; thus, it is difficult to achieve sufficient depth with them, even when the skin surface is flat. Moreover, repeated application of the gel is often needed, since the operator sweeps the US probe continuously.

Irregularities and steep slopes of a patient's skin surface can also hinder detectability. The optical markers on the US probe can be placed beyond the detectable range of the optical tracking system when the probe is swept through an irregular or steep surface. In addition, B-mode US is inherently limited by the dead zone artifacts that occur around image regions near the probe. These artifacts have been reported to depend on the probe frequency.(13)

In-house US phantom fabrications have been used for training purposes because US was originally used for diagnosis or for guiding needle insertion. To construct these US phantoms, materials have been sought that have similar properties to those of human tissue.(14-18) The relevant parameters that have been evaluated include the speed of sound, density, attenuation, and impedance in each material. Various materials have been used to make phantoms for each type of soft tissue. However, not every material has been used to make US transparent coupling materials (couplants).

To facilitate US scanning of irregular surfaces, coupling pads of various materials have been investigated.(19-22) Gel pads (pad-type acoustic coupling materials) are available commercially; however, these pads have very low viscosity, very high strength, and high cost. Moreover, these pads require additional gel to remove air bubbles and their sizes and shapes are not deformable. Therefore, a new couplant with suitable viscosity, flexibility, and variable depth and shape is needed for use in US IGRT. The ideal couplant should also make good contact and be air-free, US transparent, and cost-effective.

To overcome the aforementioned problems in US IGRT, this study aimed to develop a patient-specific 3D couplant pad with the aid of 3D printing technology. We optimized the design and composition of the pad to facilitate its use in US

IGRT. Finally, we evaluated the effectiveness of our couplant pad through phantom and patient studies.

2. Materials and Methods

2.1. Ultrasound system for IGRT

In this study, the ultrasound (US) system used for IGRT was Clarity® 3.1 (Elekta Ltd., Montréal, Québec, Canada). The Clarity system has three different handheld probes: Linear probe, Curved probe and Autoscan probe (Figure 1). The linear probe having a flat window produces 7.5MHz sound wave that can travel up to the depth of 6 cm so it is proper for a target at the shallow depth. The curved probe has a rounded window of probe and can transmit the maximum depth of 24 with using 3.4MHz. The autoscan probe that produces 5MHz sound wave is designed for transperineal scan for prostate patients. The axial resolution is 0.2 mm at the depth of 2 cm for the linear probe, 0.4 mm at the depth of 8 cm for the curved probe, and 0.5 mm at the depth of 6 cm for the Autoscan probe. The lateral resolutions at the same depths for each probe are 0.2 mm, 0.6 mm, and 1.2 mm, relatively.

The main difference between the diagnostic US and the Clarity system is the optical position-tracking system that consists of a ceiling-mounted optical camera system and the 8 infrared reflecting markers attached to the probe. This optical tracking system is necessary to calibrate the probe with respect to the room reference coordinate by using the specific US calibration phantom. During the US scanning, it detects the marker position and determines the target location.

The Clarity system is installed in both a CT simulation room and a LINAC treatment room (Figure 2). The CT simulation scanner and the LINAC system

which were used in this study were Philips Brilliance Big Bore 16-slice CT-simulator (Philips Healthcare, Cleveland, OH, USA) and Elekta Infinity™ (Elekta AB, Stockholm, Sweden).

While previous BAT systems employed image fusion between US and CT simulation image during localization, the Clarity system uses the US images as a reference to avoid the inter-modality error during image registration. The initial US scan is performed at the CT center position by using the Clarity Sim in the CT simulation room in order to define the reference target volume position. On the Clarity AFC Workstation, the target positioning reference is defined with the CT image fusion for reviewing. In the treatment room, the daily US scan is performed using the Clarity Guide system and the target position shift is calculated after the image registration with the reference image from the Clarity Sim.

(a) Linear US probe

(b) Curved US probe

(c) Autoscan US probe

Figure 1. US probes of Clarity system for IGRT

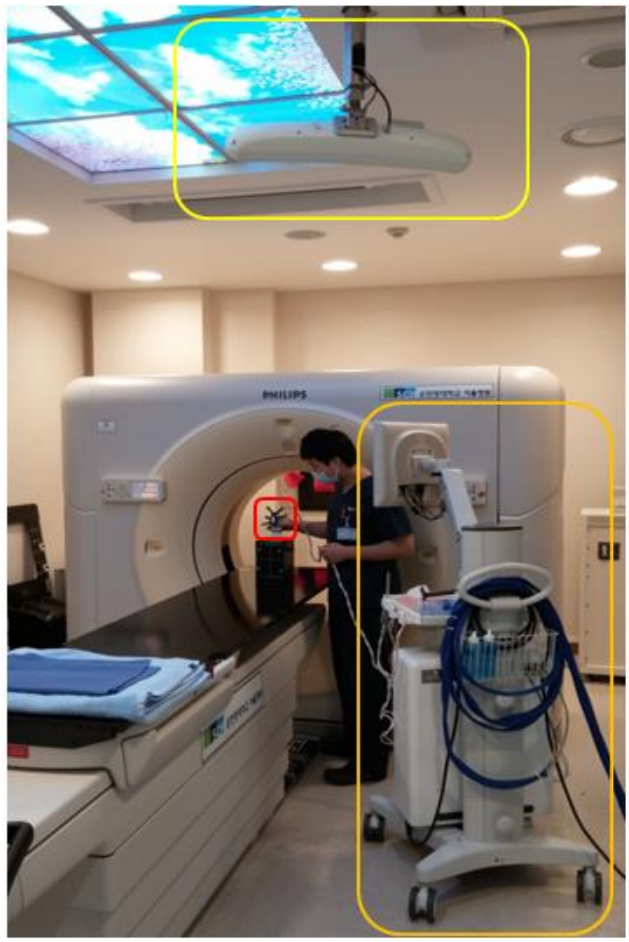

(a) Clarity Sim system installed in CT simulation room

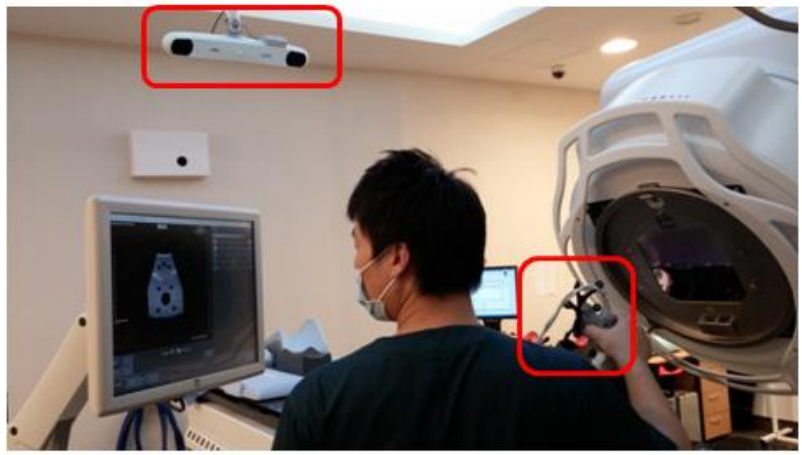

(b) Clarity Guide system installed in LINAC treatment room

Figure 2. Clarity systems installed in CT simulation room and LINAC treatment room (Clarity Sim and Clarity Guide)

2.2. Materials for couplant pad

The US coupling material (or couplant, hereafter) is used to remove air bubbles between the probe and the skin and thus to keep better contact between each other. If the speed of sound in the couplant medium is similar to that of human tissues, no acoustic interface between couplant and skin will be produced. Desirable tissue substitutes with transparent material and similar property to that of human tissues in US imaging are agarose-based, gelatin-based, magnesium silicate-based, oil gel-based, open cell foam-based, polyacrylamide gel-based, polyuerethane, polyvinyl alcohol-based, tofu, water-based, condensed milk-based, urethane rubber and zerdine.(23) In order to increase the homogeneity, water-based or polymer-based materials can be used.

The clear US image can be acquired by using couplant with low attenuation and homogeneous material. Since a couplant is desired to be composed of homogeneous and US-transmittable materials in order to minimize image noise and distortion, the Gelatin and Agarose among the abovementioned candidates were tested for phantom material. By varying the mixture ratio of these two materials, the optimal ratio for a phantom and a couplant pad was investigated by evaluating strength, elasticity and preservation period.

2.3. Phantom study

For a phantom study, a breast phantom was fabricated with the compound of gelatin and agarose and the couplant pad (CP) was fabricated with gelatin only (Figure 3). The CT and US images of the breast phantom and the CP were acquired. In order to simulate target/tumor tissue inside the phantom, agarose, commercial jelly bear and gel pad (Aquaflex, Parker Laboratories, INC., Fairfield, NJ, USA) were tested. US scanning was performed in four different sweeping directions on the CP. To achieve a better contact between the phantom and the CP, various acoustic coupling materials such as conventional US gel, mineral oil and silicon ointment were tested. The mixing ratio of materials for breast phantom and couplant pad was tested in order to determine the optimal ratio. Uniformity and image contrast were evaluated by comparing the pixel values (-1000 to 3095, -1000 shows black and 3095 shows white) on CT and US images. The target shapes were delineated and compared between cases with and without the CP.

A surgical clip was inserted into the surface center of the breast phantom. As listed in Table 1, the twenty intentional table shifts in left-right (LR), anterior-posterior (AP) and inferior-superior (IS) direction were applied to evaluate the positioning accuracy of the US-based localization with and without CP.

Figure 3. A breast phantom and a couplant pad for the phantom study

Table 1. Intentional table shifts in left-right (LR), anterior-posterior (AP) and inferior-superior (IS) direction for evaluating the positioning accuracy of US system

LR (mm)	AP (mm)	IS (mm)
0	0	0
2	1	3
5	4	6
8	7	9
11	10	12
14	13	15
17	16	18
20	19	21
1	1	1
2	2	2
3	3	3
5	5	5
7	7	7
10	10	10
15	15	15
20	20	20
25	25	25
30	30	30
5	3	10

10	5	3
3	10	5

2.4. Patient study

Among the subjects eligible for US IGRT, six patients were selected in this study to evaluate the effectiveness of the developed CP. The lesions undergoing treatment were targets near skin or under an irregular surface. Exclusion criteria of the patients in this study are as follows: (1) Prostate cancer patients undergoing transperineal scanning with AutoScan probe; (2) Patients with targets not detectable in US images; (3) Patients allergic to gelatin and mineral/vegetable oil; (4) Patients who have a possibility of infection on target region. Two patients volunteered for this study prior to the institutional review board (IRB) approval and four patients participated in the study after the approval (IRB number 2014-11-029). The first volunteer was a breast cancer patient and the hand-made couplant pad was applied to US scanning. The second volunteer was a parotid cancer patient and a patient-specific 3D couplant pad was fabricated using the patient skin mold by using 3D printing technique.

The target of the first patient (patient 1) was an inguinal lymph node and the patient had an irregular surface. The second patient (patient 2) also had a treatment of an inguinal lymph node and the target was placed at the depth of about 2 cm. The third patient (patient 3) was a tonsil cancer patient and due to the target location the probe movement had a difficulty that the probe marker was not detectable by shoulder. The fourth patient (patient 4) had a target at the shoulder that was placed underneath the irregular surface at the shallow depth from skin and it was difficult to give a pressure to the probe due to bone. The curved probe was used for the first and third patients and the linear probe was used for the second and fourth patients.

The treatment prescription of patient 1 and patient 2 were 60 Gy (2 Gy per fraction) and the PTV margins were 5 mm. It was 67.5 Gy (2.25 Gy per fraction) with the PTV margin of 3 mm for patient 3 and 74 Gy (2 Gy per fraction) with the PTV margin of 5 mm for patient 4. For all patients, the x-ray image acquisition was performed before the treatment by using the CBCT (minimum once a week and maximum twice a week) and the kV planar imaging (maximum twice a week). The US scanning was performed daily before the treatment and the x-ray imaging.

The general procedure of the US IGRT is shown in Figure 4. Both the simulation CT and US images are acquired in the simulation room. These images are fused and the target is delineated on the US Sim image. However the dose calculation for the treatment planning is based on the electron density of CT image. Before the treatment, the US scan is performed in the treatment room and registered with the US sim image. The patient target position shift is calculated. If necessary, the patient is repositioned. If the target is within the tolerance (such as PTV margin), the treatment is started. However, if the target position is out of the tolerance or the target volume/shape is significantly different from the reference target volume/shape, the procedure is repeated from the image acquisition for the adaptive radiation therapy.

A new procedure of the US IGRT with applying the couplant pad developed in this study is shown in Figure 5. In addition to the general procedure of US IGRT, the US scan with using the couplant pad was included. During the simulation US image acquisition, the couplant pad could not apply to the patient. On the simulation CT image, the patient's skin contour covering the target volume was extracted. During the treatment planning, the patient's skin model was made by using the 3D printer. On the skin model, the patient-specific couplant pad based on

gelatin was developed. Before the treatment in the treatment room, the couplant pad was applied to the patient and the US image was obtained with the couplant pad. Each daily US image was registered with the first US image with using the couplant pad.

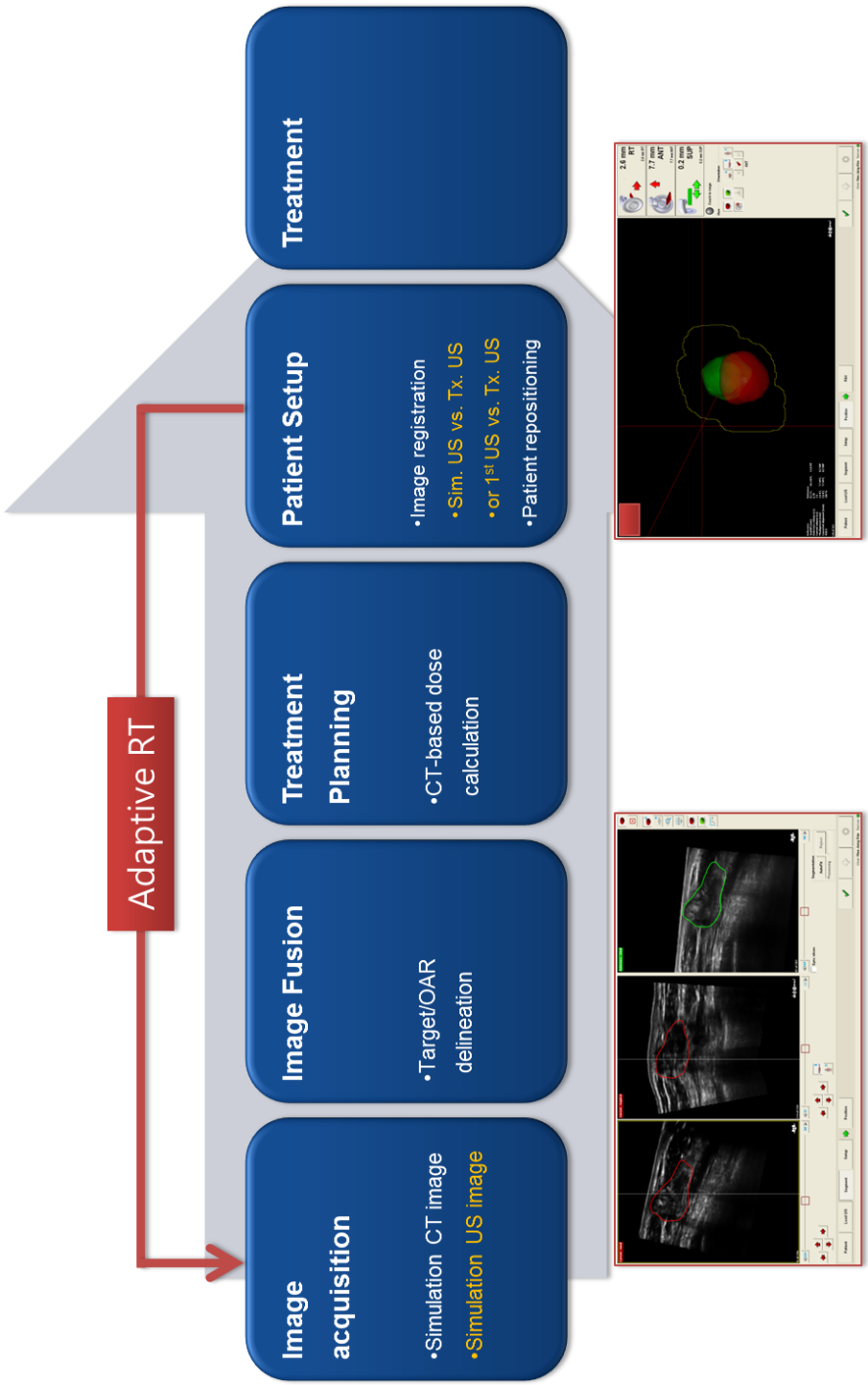

Figure 4. A general process of US IGRT

Figure 5. A new process for US IGRT with applying the couplant pad

2.5. Development of couplant pad

The CP was made with using the optimal mixture ratio found from the phantom test. The couplant pad making process is as follows: 1) MIM® (MIM Software Inc., Cleveland, OH, USA) software was used for contouring the skin including the treatment target on the CT images and exporting as a dicom file. 2) The dicom file for the patient skin contour was imported to the 3D Slicer (BWH and 3D Slicer contributors) software which makes skin surface model using SlicerRT module and converts it to the STL file format for the 3D printing.(24,25) 3) By using 3D printer (CubePro® , Cubify, 3DSYSTEMS, Rock Hill, SC, USA), the patient skin model for the area where is scanned by US was made using PLA (Polylactic acid). 4) The edible gelatin powder was mixed with hot water and 83% Ethanol as a preservative with the ratio 1:5:0.5. 5) The patient skin model was fixed in the container. The gelatin solution was poured into the container and put it in the refrigerator during 2 hours to solidify to be a couplant pad. The couplant pad was separated from the container and the patient skin model. The minimum depth (t in Figure 6) of the couplant pad should be 1 cm or more. 6) After spreading oil (mineral or vegetable) inside the couplant pad or on the patient skin, the couplant pad was put on the patient (see Figure 6) and the US scan was performed.

For four patients, US images were acquired before the treatment by the three different users (one physicist, two therapists) in both conditions with and without applying the couplant pad.

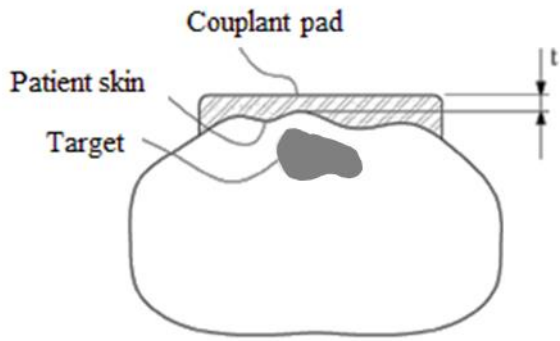

Figure 6. Couplant pad application to the patient (in axial view)

2.6. Data analysis and statistics

The target was contoured on the US images and the volume was calculated. The image contrast which is a pixel value difference between the target and the area of 1 cm away from the target was calculated. The equations to calculate the contrast are as follows:

$$\text{Contrast (pixel value)} = |\text{Mean value of target} - \text{Mean value of surrounding medium}| \quad \text{(Eq. 1)}$$

$$\text{Contrast difference (pixel value)} = \text{Contrast}_{with\ CP} - \text{Contrast}_{without\ CP} \quad \text{(Eq. 2)}$$

$$\text{Contrast difference (\%)} = \frac{\text{Contrast}_{with\ CP} - \text{Contrast}_{without\ CP}}{\text{Contrast}_{without\ CP}} \times 100 \quad \text{(Eq. 3)}$$

where $\text{Contrast}_{with\ CP}$ and $\text{Contrast}_{without\ CP}$ are the pixel values of the contrast (Eq. 1) of the US image with and without applying the CP.

Inter-operator variation from which conventional US IGRT has suffered was also evaluated. The equation for target volume difference and the standard error (SE) are following.

$$\text{Target volume difference (\%)} = \frac{\text{Target volume}_{N^{th}\ US} - \text{Target volume}_{1^{st}\ US}}{\text{Target volume}_{1^{st}\ US}} \times 100 \quad \text{(Eq. 4)}$$

where Target volume$_{1^{st}\ US}$ and Target volume$_{N^{th}\ US}$ are the target volume of the US image acquired in the first treatment session (1st US) and the Nth US image.

All US images was registered to the 1st US image and the value of target position shift was computed. After image registration, the centroid of target volume was compared so that the target volume variations depending on the US scanning coverage of target and the target deformation are evaluated.

Using SPSS softwaere, the statistical analysis was performed with paired t-test and linear mixed model to investigate the effectiveness of the developed CP in terms of image contrast and inter-user variation. In order to evaluate the target contour consensus depending on the use of the CP, Computational Environment for Radiotherapy Research (CERR) software was used and the kappa value was calculated.(26,27) Kappa value can be calculated by the following equation (Eq. 5)[15] and shows an agreement between the contours (Table 2).(28)

$$\text{kappa value} = \frac{apparent\ agreement - chance\ agreement}{chance\ agreement} \quad \text{(Eq. 5)}$$

Table 2. Descriptive scale of kappa value

Kappa value	Agreement
<0	Less than chance agreement
0.01-0.20	Slight agreement
0.21-0.40	Fair agreement
0.41-0.60	Moderate agreement
0.61-0.80	Substantial agreement
0.81-0.99	Almost perfect agreement

Although the Clarity is an intra-modality system, the inter-modality variation was evaluated in this study, by comparing the position shift between the simulation CT image and the US image. The difference of the patient positioning between the CBCT registration result relative to the simulation CT and the US registration result relative to the first US image. These results were compared with the inter-modality result that the target contours of the US fractional images were compared to the target contour of the first US image.

3. Results

3.1. Couplant pad material

The CT and US images for agarose, gelatin and commercial jelly bear were acquired (Figure 7). In the CT images, both gelatin and agarose looked similar and the pixel values were above 10. In the US images, the agarose had a standard deviation (SD) of 118 and showed like heterogeneous material such as a human tissue. However the gelatin inside showed a dark with the pixel value of -1000 like air and it was homogeneous with the SD of 1 pixel value, except the interfaces. (Table 3) For the commercial jelly bear, CT showed a clear image with low SD and high pixel value but the US images showed like a material more heterogeneous than the agarose and showed a shadow below that. The result of the target volume change depending on the US scanning direction was less than 0.1cc.

Based on above results, the gelatin was selected for the couplant pad. To make the couplant pad, gelatin, hot water and 83% ethanol were mixed. From the result of various tests for the mixture ratio, the optimal ratio considering the strength and elasticity was gelatin (100 ml), hot water (500g) and 83% ethanol (50g).

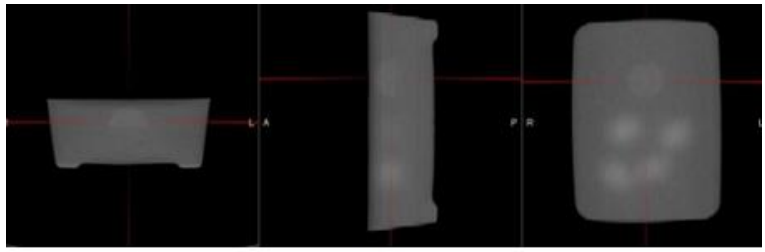

(a) CT image

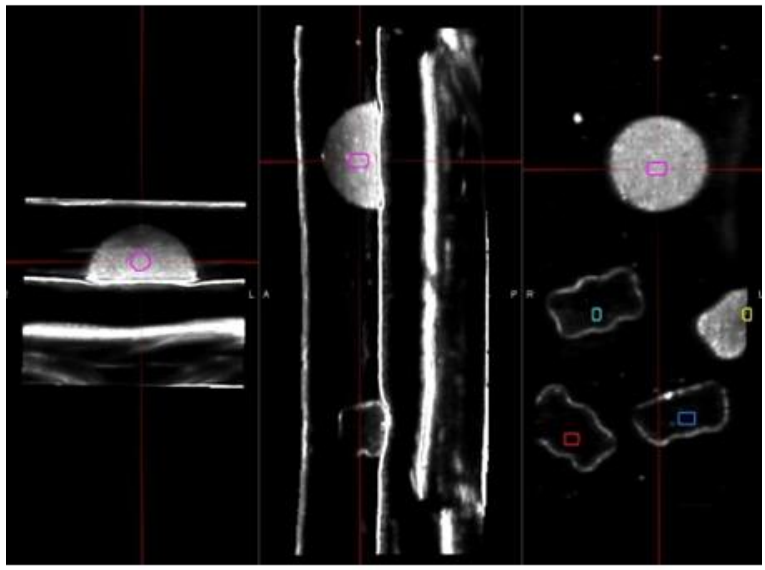

(b) US image

Figure 7. CT and US images of various materials for making a couplant pad

Table 3. Image uniformity of phantom materials in terms of average and standard deviation of pixel value with the range from -1000 (black) to 3095 (white)

	CT	US
Gelatin	16 ± 3	-1000 ± 1
Agarose	13 ± 3	-280 ± 118
Jelly Bear	323 ± 7	-620 ± 245

3.2. Phantom study result: Image contrast

For the breast phantom, the mixture of gelatin and agarose was used as a breast tissue and the gel pad piece was inserted as a target. The couplant pad was made with gelatin only. The CT and US scan of the breast phantom with and without the couplant pad were performed. (Figure 8)

Since the target was positioned underneath the breast phantom surface, the volume of target contour had a difference between image modalities depending on the use of the CP. (Table 4) The target volume was larger in CT than in US. When the couplant pad was applied, the target volume was increased, compared with when the couplant pad was not applied.

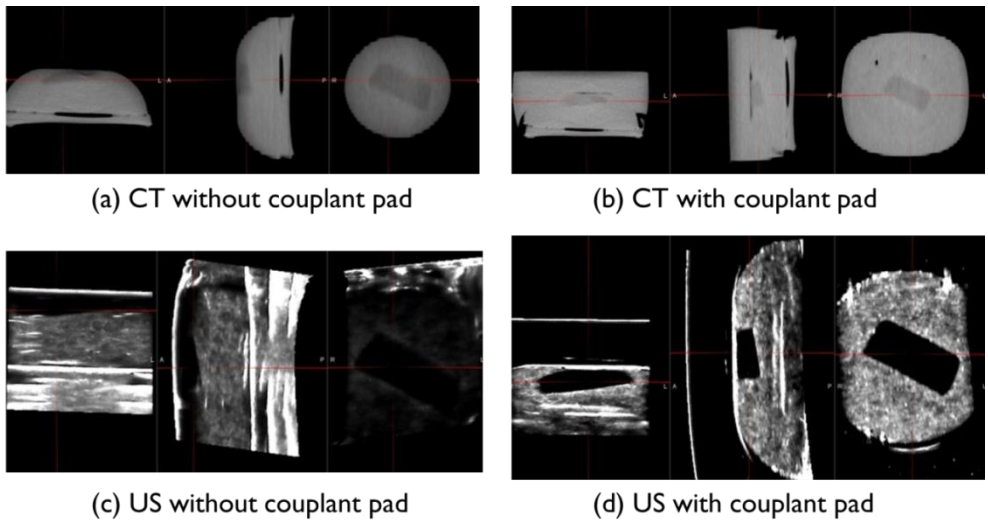

Figure 8. Phantom test images using CT and US

Table 4. Phantom target volume delineation

	CT		US	
	without CP	with CP	without CP	with CP
Target volume (ml)	5.9	6.4	4.3	5.5

The target of the breast phantom and the spheres as surround tissues with 1cm diameter 2cm away from the target were delineated and the pixel values were compared. In CT images, the image contrast, a difference of pixel values between the target and the spheres, was 24 pixel value higher when the couplant pad was not applied than when the couplant pad was applied. (Table 5) However, in US images, it was 80 pixel value higher when the couplant pad was applied. In the images both with and without the use of the couplant, US scan showed the image contrast of about 10 times higher than CT scan.

Table 5. Image contrast in phantom test in terms of mean pixel values of target and surrounding volumes

	CT		US	
	without CP	with CP	without CP	with CP
Target	-25	3	-999	-942
surrounding	9	13	-687	-550
Difference	34	10	312	392

3.3. Phantom study result: US positioning accuracy

A surgical clip was positioned at the center underneath the breast phantom surface. During twenty intentional table shifts, the mean 3D vector amplitude of a surgical clip positioning discrepancy was decreased by 0.4 mm due to the use of CP. (Table 6) In anterior-posterior (AP) direction, the clip position at the center on the surface of the phantom was shifted by 1 mm on average when the CP was not applied. However it was decreased by 0.4mm on the US scan with CP and this was statistically significant with p-value of 0.012. The 1 standard deviation (SD) was less than 0.5 mm in both US scans with and without CP.

Table 6. Accuracy of US image guidance system used in RT : positioning errors from phantom test with intentional table shifts depending on the use of couplant pad (CP)

	without CP	with CP
LR (mm)	-0.2 ± 0.3	-0.4 ± 0.4
AP (mm)	-1.0 ± 0.4	-0.6 ± 0.3
IS (mm)	-0.6 ± 0.4	-0.4 ± 0.4
3D (mm)	1.3 ± 0.4	0.9 ± 0.3

3.4. Patient study result: manual

The hand-made CP was applied to the first volunteer patient with a breast cancer. The US scans with and without the CP were performed and the resulting images were compared to the simulation CT images. As shown in Figure 9, when the couplant pad was not applied, a notable deformation of the skin surface was observed since the linear probe made the patient surface flat. Moreover, multi path artifacts were also observed due to the changes of the scanning speed and direction of the probe to deal with irregular surfaces. When the CP was applied, the skin surface was preserved intact on the US image and was matched well with the simulation CT.

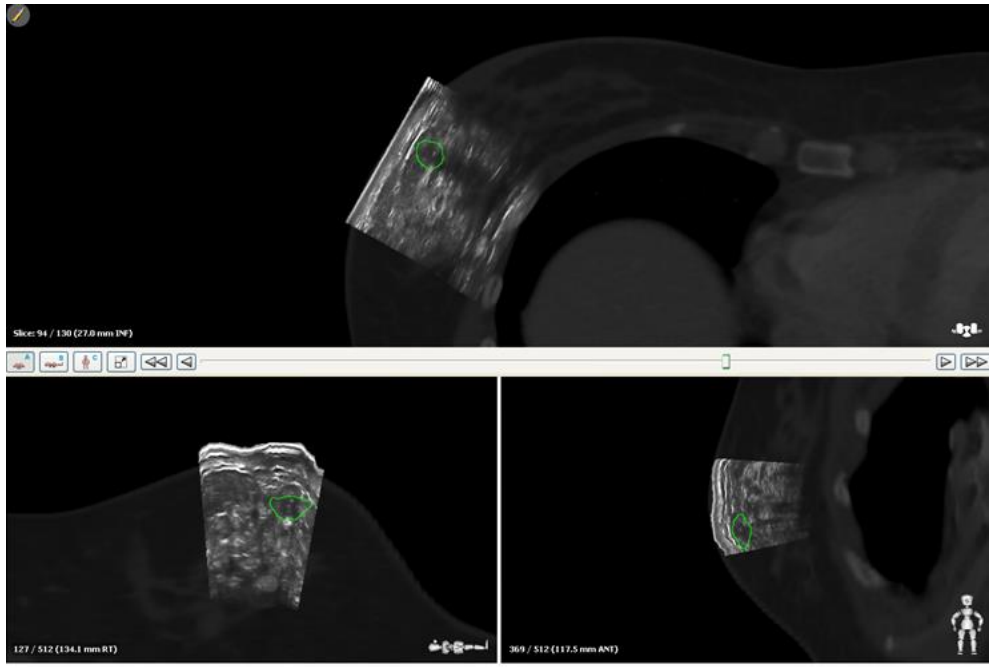

(a) CT fused with US image without a couplant pad

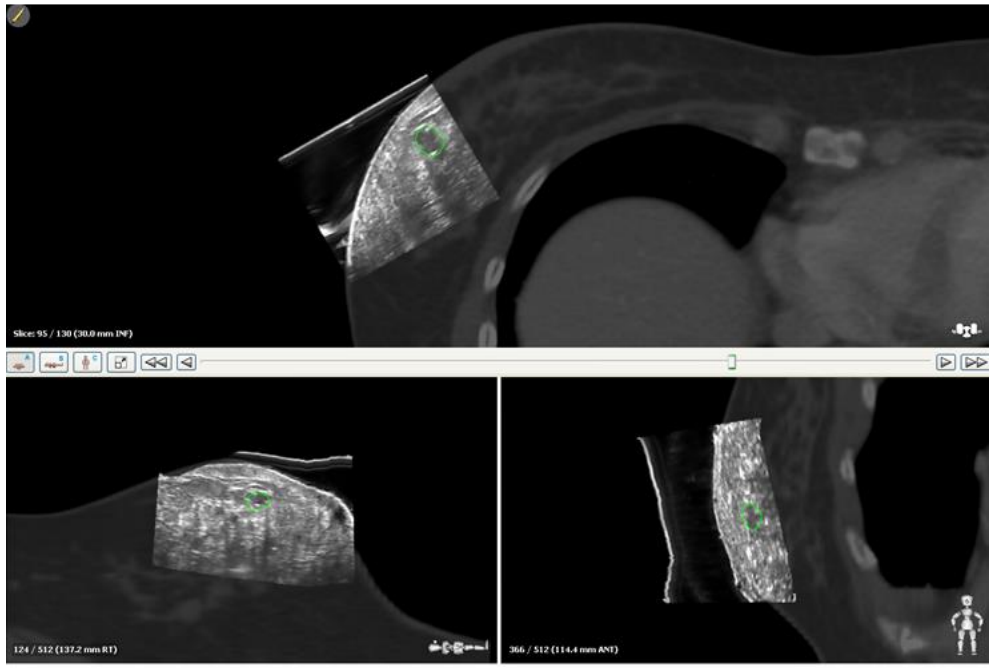

(b) CT fused with US image with a couplant pad

Figure 9. Fused image of CT and US images for volunteer 1 (breast case), with and without a couplant pad

3.5. Patient study result: 3D printing

For the second volunteer patient with parotid cancer (Figure 10), the patient skin mold produced by 3D printer was used in order to make the CP and the US scan was performed. Since the treatment target was near left ear and underneath skin, the linear probe was used. When the CP was not applied, large amount of US coupling gel was needed in order to minimize the probe pressure due to the shallow depth of the target from the skin. In addition, the irregularity of surface was excessive so US scan could not cover the whole target volume area and the dark shadow due to the air was shown around the target. However, when the CP was applied, there was no difficulty for scanning. Moreover, the patient skin was shown clear in US image so it was easy to fuse the images and to delineate the target.

Including the second volunteer, three patient cases except the second patient (inguinal lymph node) applied the 3D printed-patient skin mold extracted from the skin contour on the simulation CT images (Figure 11).

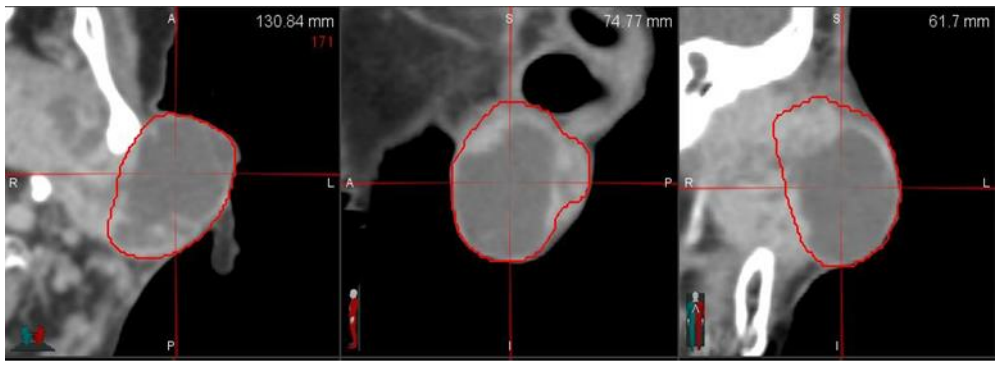

(a) Simulation CT

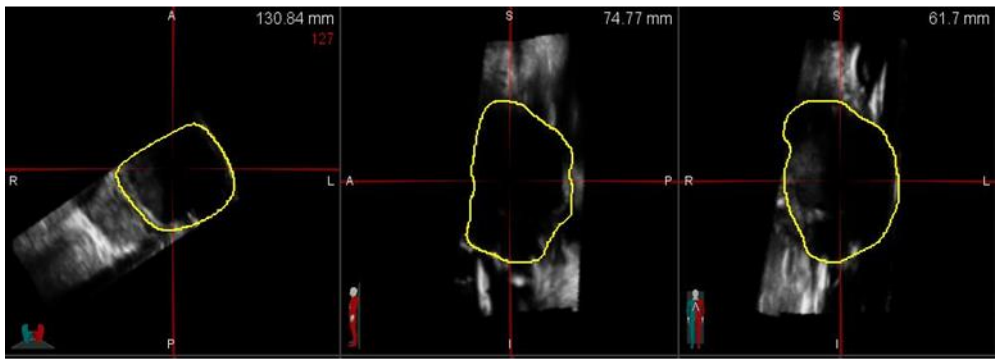

(b) US without the couplant pad

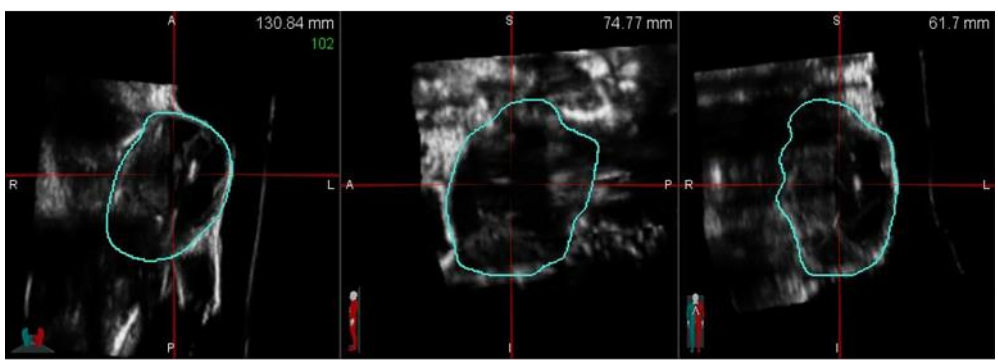

(c) US with the couplant pad

Figure 10. Image registration of (a) Simulation CT and US images (b) without the couplant pad and (c) with the couplant pad for volunteer 2 (parotid case)

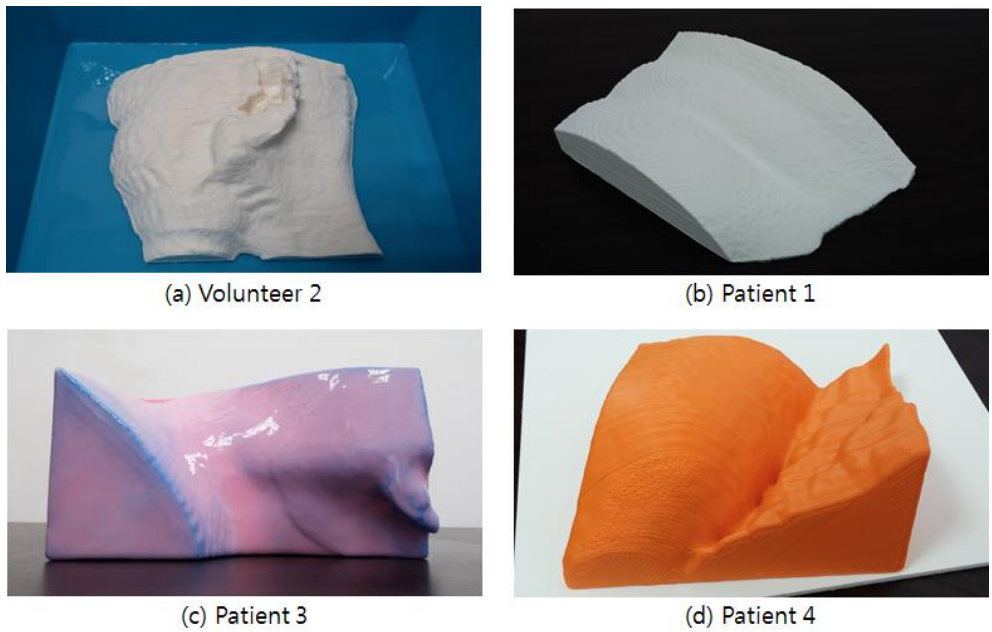

Figure 11. Patient skin mold fabricated by a 3D printer using the skin contour of the simulation CT images

3.6. Patient study result: interfractional displacement

Figure 12 shows the patient setup for US scan without the couplant pad (CP) and with the CP for patient 1, patient3 and patient 4 who were used the 3D CP using the molds by 3D printing technique. For four patients, 4 simulation CT images and 486 US images were acquired. (Figure 13) The US images were registered to the first US image. The target position shift in left-right (LR), anterior-posterior (AP) and inferior- superior (IS) directions was evaluated. In the registration result of the US relative to 1^{st} US (Table 7), both the average and 1 standard deviation (SD) were smaller in the result of the US scan with the CP than in the result of the US scan without the CP in all directions and its difference was statistically significant ($p < 0.001$) except the data in LR direction. In AP direction, mean shift was decreased by 0.9 mm due to the use of CP. In all directions, the mean target position shifts of the US scan with using CP were less than 1 mm that there was no systematic error in US scan procedure including the US system calibration and room laser calibration.

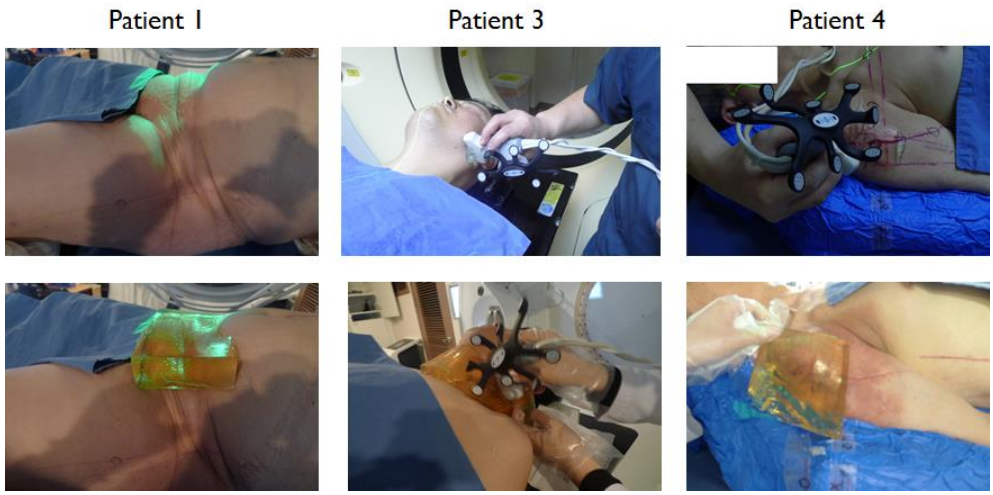

Figure 12. Patient setup for US san without the couplant pad (upper row) and with the couplant pad (lower row)

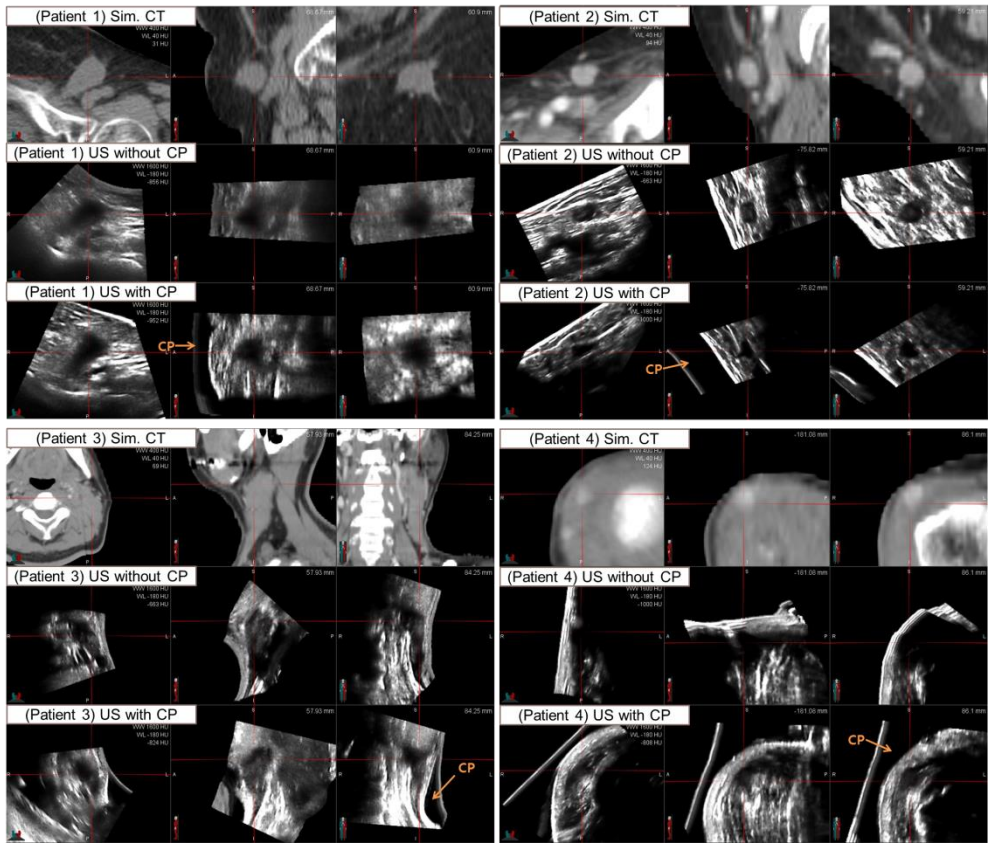

Figure 13. Simulation CT and US images of the four patients

Table 7. Target position shift difference between the US scan with and without couplant pad (CP). The target position shifts were calculated by subtracting the target position of the first US image which was used as a reference image.

	without CP	with CP	*p*-value
LR (mm)	0.8 ± 3.6	0.8 ± 3.3	0.996
AP (mm)	-1.8 ± 1.9	-0.9 ± 1.6	<0.001
IS (mm)	-0.7 ± 2.5	0.6 ± 1.4	<0.001
3D (mm)	4.7 ± 2.2	3.7 ± 1.7	<0.001

3.7. Patient study result: image contrast

The target was delineated and compared with the surrounding tissue that was a 1cm thickness shell around the target. The target volume and image contrast were calculated.

As listed in Table 8, the result from total 324 US images shows the statistically significant increase in image contrast due to the use of CP. The image contrast was increased by 10% overall regardless of the users.

Table 8. Image contrast increase in US scans with the couplant pad (CP), compared to the image contrast without CP

	Median (pixel value)	Percentage	*p*-value
user 1	52	13%	0.005
user 2	25	5%	0.001
user 3	38	12%	0.003
Total	37	10%	0.001

3.8. Patient study result: target volume contouring variation

Target volume contouring variations among the different users depending on the use of CP were evaluated in terms of standard deviation (SD).

As listed in Table 9, the target contouring variations in the US scan without CP were maximum 19% depending on the user handling of US scan. However, it was decreased by minimum 2% to maximum 16% in all patients due to the use of CP and overall median SE was also decreased by 3% ($p = 0.001$).

Table 9. Target volume contouring variations among the different users depending on the use of couplant pad (CP) in terms of median value of standard deviations (SD)

	without CP	with CP	*p*-value
Patient 1	8%	4%	0.002
Patient 2	5%	3%	0.672
Patient 3	15%	7%	0.287
Patient 4	19%	3%	0.038
Total	7%	4%	0.001

3.9. Patient study result: centroid of target volume

After image registration based on the 1st US image, the centroids of target volumes were calculated in order to analyze the correlation between the centroid of target volume and the use of CP. The centroid of US scan without CP was not close to zero in AP direction that the shift was 2.1 mm on average (Table 10). However, in the US scan with CP it was less than 1 mm in all direction. The standard deviation (SD) was smaller in the US scan with CP than in the US scan without CP. The mean and SD of 3D vector amplitude of the centroid was decreased by 1.3 mm and 0.9 mm due to the use of CP, relatively. This effect of the use of CP in the centroid of target volume was statistically significant in LR, AP and 3D vector with *p*-value less than 0.001 for the linear mixed model.

As listed in Table 11, the correlation of the centroid of target volume among the three different users was also evaluated by using the linear mixed model. Depending on the user handling, the centroid was significantly different ($p < 0.05$ in all direction) only when the US scan was performed without using CP.

Table 10. Centroid of target volume after target position alignment: Analysis of the correlation between the centroid of target volume and the use of couplant pad (CP) by using linear mixed model

	without CP	with CP	*p*-value
LR (mm)	-0.7 ± 2.1	0.1 ± 1.7	< 0.001
AP (mm)	2.1 ± 2.8	0.7 ± 1.7	< 0.001
IS (mm)	-0.4 ± 4.2	-0.6 ± 3.3	0.218
3D (mm)	4.4 ± 3.9	2.9 ± 3.0	< 0.001

Table 11. Centroid of target volume after target position alignment: Analysis of the correlation of the centroid of target volume among the three different users by using linear mixed model

		User 1	User 2	User 3	*p*-value
without CP	LR (mm)	-0.7 ± 2.2	-0.2 ± 2.1	-1.2 ± 2.0	0.005
	AP (mm)	2.1 ± 2.8	1.5 ± 2.3	2.6 ± 3.2	0.002
	IS (mm)	0.2 ± 4.7	0.5 ± 3.9	-1.8 ± 3.5	<0.001
	3D (mm)	4.5 ± 4.4	3.9 ± 3.5	4.8 ± 3.8	0.020
with CP	LR (mm)	-0.0 ± 1.4	0.3 ± 1.7	0.1 ± 1.8	0.081
	AP (mm)	0.5 ± 1.4	0.7 ± 1.5	0.8 ± 2.2	0.582
	IS (mm)	-1.0 ± 3.2	-0.6 ± 3.2	-0.4 ± 3.5	0.194
	3D (mm)	2.7 ± 2.9	2.8 ± 2.9	3.3 ± 3.2	0.133

3.10. Patient study result: target contour consensus

Figure 14 shows the target contouring on the simulation CT and US images for 4 patients. The target volume deformation was evaluated by using the kappa value. The consensus of target volume contours after image registration was calculated depending on the user and the use of the couplant pad. (Table 12)

For the patient 1, 2 and 3, all kappa values were over 0.61 (good agreement). For the patient 4, the kappa values in the US without the couplant pad were less than 0.07 (poor agreement). However, the strength of agreement increased due to the use of the couplant pad and the kappa values were over 0.31 (fair agreement).

Table 12. Kappa values for contour agreement depending on the user and the use of couplant pad (CP)

		Patient 1	Patient 2	Patient 3	Patient 4
User 1	without CP	0.75	0.74	0.54	0.07
	with CP	0.7	0.67	0.65	0.32
User 2	without CP	0.72	0.79	0.65	0.04
	with CP	0.7	0.71	0.65	0.22
User 3	without CP	0.75	0.76	0.68	0.04
	with CP	0.71	0.68	0.67	0.26
Total	without CP	0.74	0.77	0.63	0.07
	with CP	0.71	0.71	0.67	0.31

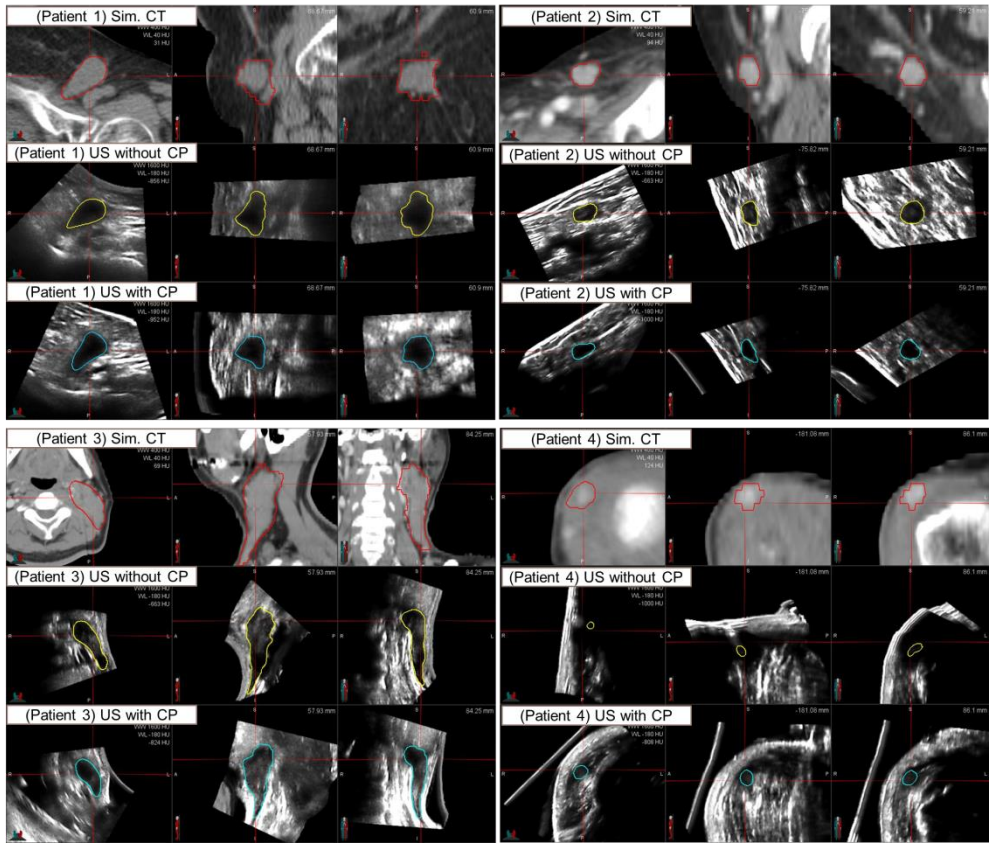

Figure 14. Target volume contours on the simulation CT and US images of the four patients

3.11. Patient study result: target volume change during treatment

In the second patient, the target volume had been changed during the radiation treatment (Figure 15). In the target volume, there was an inter-modality difference between the simulation CT and the ultrasound, as the results of literatures(29-32). The target volume on the simulation CT image was 1.2 cc. At the first day of the treatment, it was 0.77 cc on the US image without the CP and 0.69 cc on the US image with the CP. After 23 fractions of the treatment, the target volume decreased by 0.28 cc (37%) and 0.40 cc (57%) on the both US images without the CP and with the CP (Figure 16).

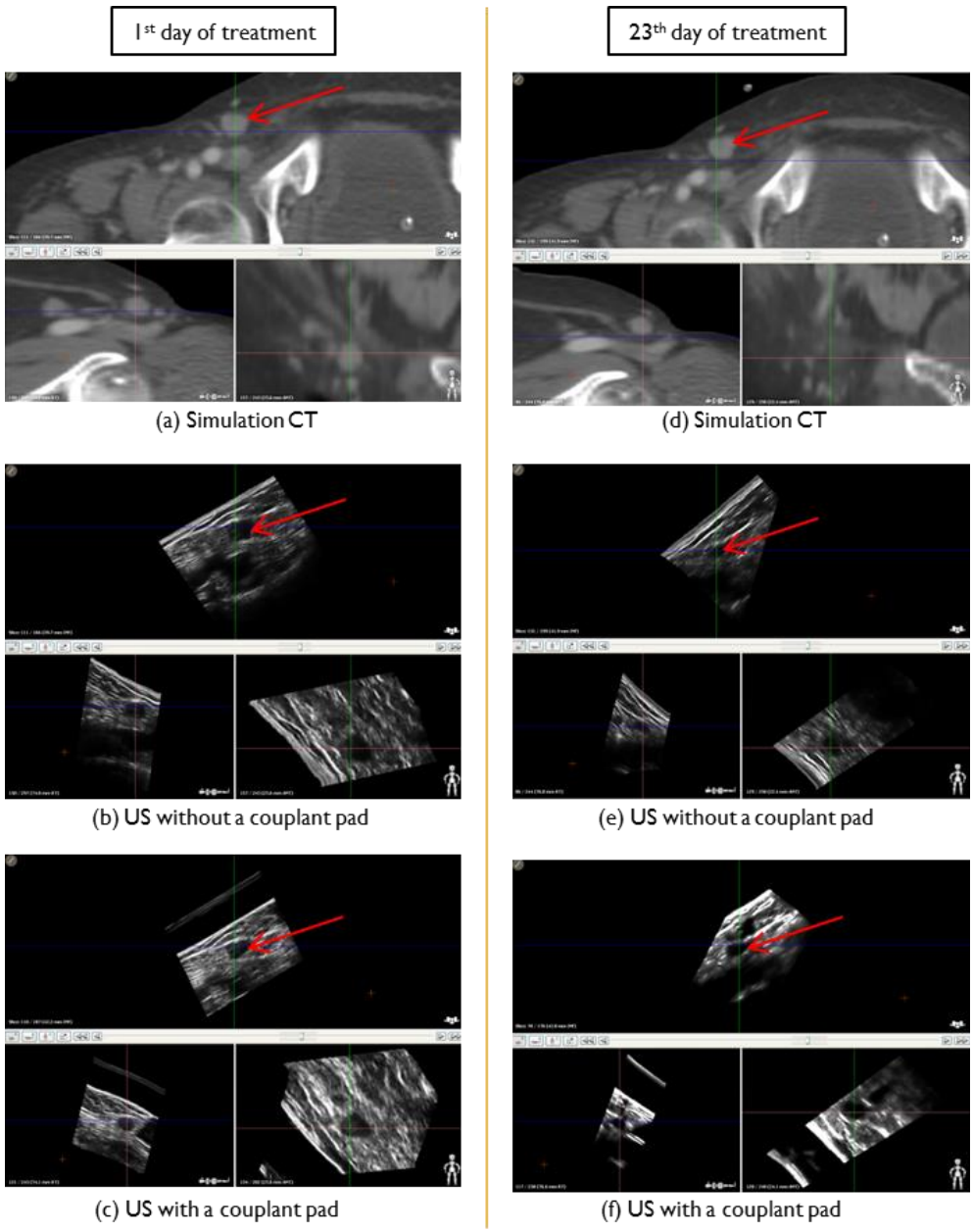

Figure 15. Target volume difference between the first day of the treatment and the 23th fraction of the treatment of patient 2 on the simulation CT image and the US images without and with the couplant pad

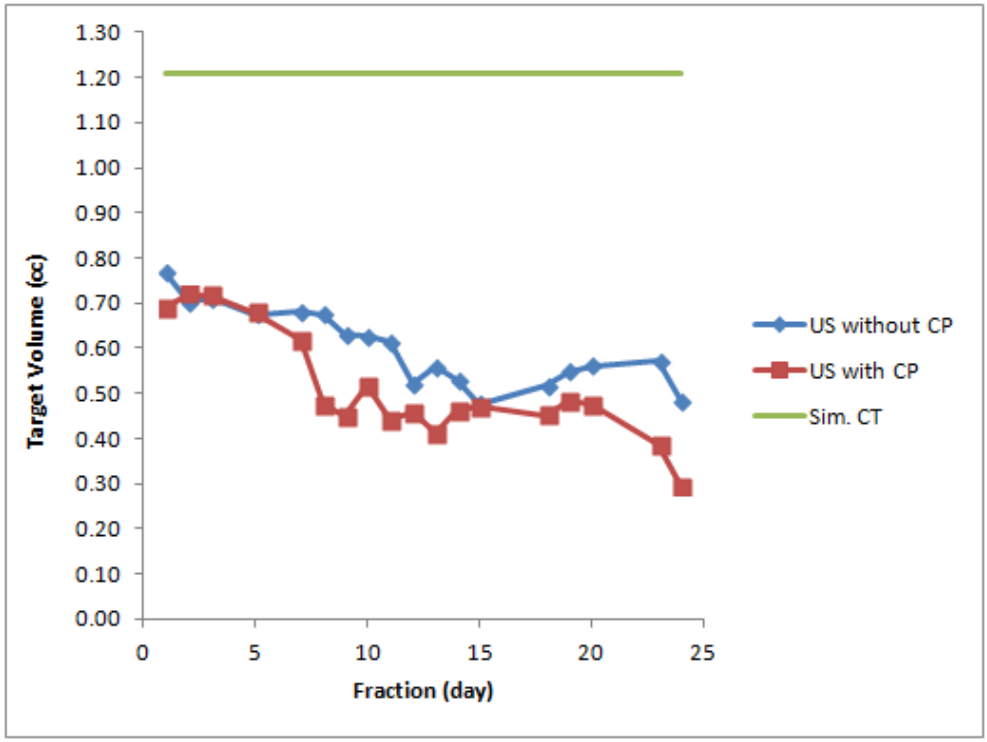

Figure 16. Decrease of target volume during radiation treatment in patient 2

3.12. Patient study result: inter-modality variation

The target contours of the US images were registered to the target contour of the simulation CT image. Total 324 US images were fused to the simulation CT images and the registration results are listed in Table 13. The standard deviations of the positioning shifts were maximum 1.2 mm greater than the result in Table 6. The 3D vector amplitude was decreased by 1 mm (p-value < 0.001) due to the use of CP in the result of inter-modality registration (US vs 1^{st} US), but it was not significantly different in the result of inter-modality registration (US vs. simulation CT).

The US positioning shift results which were registered to the 1^{st} US image were compared to the registration results of the CBCT relative to the simulation CT. The 18 CBCT images acquired when the US scan was performed both with and without using the couplant pad were used for analyzing the image registration difference. As listed in Table 14, the difference between the CBCT image guidance and the US image guidance was 4 mm on average regardless of the effect of the couplant pad.

Table 13. Inter-modality variation, comparing the target contours of the reference simulation CT image to US image

	without CP	with CP	p-value
LR (mm)	-0.8 ± 2.8	-1.0 ± 2.9	0.209
AP (mm)	-0.1 ± 3.0	0.5 ± 2.8	0.019
IS (mm)	-0.3 ± 2.4	-0.3 ± 1.8	0.870
3D (mm)	4.4 ± 2.0	4.2 ± 1.7	0.268

Table 14. The difference of positioning shift between the inter-modality image registration (using the CBCT image registered to the simulation CT image) and intra-modality image registration (using the US image registered to the first US image)

	without CP	with CP	p-value
LR (mm)	-0.9 ± 1.9	-0.9 ± 1.8	0.980
AP (mm)	-1.6 ± 2.6	-1.6 ± 2.9	0.980
IS (mm)	-1.3 ± 2.5	-1.3 ± 2.5	0.980
3D (mm)	4.0 ± 2.3	4.0 ± 2.7	0.988

4. Discussion

Since the Clarity US system used in this study can use US images as reference images for image registration, no inter-modality effects were present and the scanning direction effects were negligible (less than 0.1 cc). In this study, the couplant pad was made of gelatin, a homogeneous colloid gel that is produced from animal collagen. The collagen was combined with a sufficient amount of water so that the density of the couplant pad ranged from 1004 kg/m3 – 1024 kg/m3, which is similar to that of water. Thus, the speed of sound in the couplant pad may be similar to that in water (1520 m/s – 1650 m/s).(33) The gelatin was easy to use, cost-effective, homogeneous, and exhibited low acoustic attenuation. These highly desirable properties make gelatin an ideal material for a couplant pad to be used during US scanning. In the phantom study, the abilities of a conventional US gel, mineral oil, and silicon ointment to remove the air between the couplant pad and the phantom surface were tested. Conventional US gel has a higher viscosity than water or oil and did not sufficiently remove the air, whereas the interface was too bright with the silicone ointment. The mineral oil yielded a clear interface and did not make air bubbles, making this material suitable for patient studies.

As ultrasound energy travels through different tissues and materials, it is reflected at the interfaces between tissues of different densities and returns to the probe as reflected echoes.(34) The reflection is proportional to the difference in impedance. However, echoes are not produced when adjacent tissues have the same impedance. Fluids like ascites, bile, and water within cysts all appear as echo-free (sonolucent)

areas on ultrasound images. Homogeneous tissues such as hypoechoic structures have fewer interfaces, meaning that less reflection occurs. Since the couplant pad developed in this study is based on gelatin, whose properties are similar to those of water, the couplant pad appeared as an echo-free structure on the ultrasound images and was accompanied by high image uniformity.

When ultrasound waves pass through a fluid-like medium, they are transmitted with little absorption of the ultrasound energy. When a medium attenuates less than its surrounding tissue, it is seen as a hyperechoic or bright area on the far side of a fluid-filled structure; this effect is referred to as increased through transmission.(35) Ultrasound imaging noise is caused by excess gain or low gain.(36) This issue can be resolved by decreasing or increasing the overall gain. However, excessive gain can result in false echoes or oversaturation. To resolve low gain artifacts, applying more acoustic coupling material can help to increase the far gain and the overall gain. For these reasons, image contrast was increased on average by 10% in this study with the use of the couplant pad.

Many potential issues have been raised regarding the use of US systems for IGRT. The first issue is the limitations of the optical tracking range. Since the optical tracking system is fixed on the ceiling and should detect the reflective marker attached on the probe to generate the 3D US image in the same coordinates as the linac, the tracking range of the optical tracking system is limited.(37,38) In addition, the probe rotation is limited due to the marker position. Thus, the marker cannot be detected when the probe moves on steeply curved or irregular surfaces. The second issue is that copious US gel and careful probe movement must be applied in order to minimize probe pressure when the target lies underneath the skin or under an irregular surface.(39) Even if high viscosity US gel is used, it can

spill because of the slope of the steep curved surface. Thus, the US gel will potentially have to be reapplied after only one sweep of the probe. Third, when scanning on curved surfaces, the direction and speed can change and multi-path averaging artifacts can occur. The fourth issue is dead zones, which occur due to the inherent technical properties of the US probe. When the treatment target is close to the skin, it is difficult to clearly identify the target boundary. To bring the target into the focal zone (geometric focus) of the probe and out of the dead zone, commercial gel pads can be of use.(19,22,40,41) Gel pads have been demonstrated to have long life spans and their acoustic properties are appropriate for coupling materials.(19-22) However, the major drawback of gel pads is their inability to adequately cover curved surfaces. Moreover, these pads come in only standard sizes, thicknesses, and shapes.

The patient-specific 3D couplant pad developed in this study solves these problems. The specific contour of each patient's skin is used to make the mold for the couplant pad. Since the couplant pad has a flat surface on the side on which the probe moves, the marker is always detectable without a dead angle. The gel is used only for the probe surface, thus no US gel is wasted. In addition, the couplant pad is placed on the same position of the patient's skin. Thus, the time required to perform a US scan and apply the couplant pad is about 3 min, which is less than the total time required for a conventional US scan using US gel without a couplant pad. The mean US target volume shift in our study was 1.8 mm without the couplant pad and 0.9 mm with the couplant pad. Moreover, the couplant pad significantly reduced inter-observer variation in US scanning. However, this finding was based on 486 images from only 4 patients and additional images and patients will be required to determine the PTV margin for US IGRT.

The couplant pad developed in this study is easy to make, requiring only 3 hours from the extraction of patient's skin contours to the generation of the final couplant pad. In this study, the use of couplant pads during simulation CT scans was limited since the simulation CT images had to be used to make the couplant pads. If the resimulation CT and simulation US images using the CP are acquired at the same time before the treatment, the simulation US image can be used as a reference US image. Alternatively, a 3D scanner can be used before the simulation CT / US. If it is feasible to make a patient-specific CP before the simulation CT/US scan, the CP will be available during the simulation and the image from the US simulation with the CP can be used as a US reference image. If the patient's position is corrected by CBCT and the US image initially obtained in the treatment room is used, the first US image can be used as a reference image for the image registration instead of the simulation US image.

In the second patient, the target volume changed during the radiation treatment. Specifically, the volume decreased and the shape changed. However, the couplant pad enabled very clear images to be obtained, thus yielding accurate target delineation. The couplant pad was also helpful for detecting precise changes in target volumes. In contrast to x-rays, US scans can be performed every day, including before, during, and after treatment. An important advantage of US scans is that the target volume and shape can be monitored every day without extra radiation doses. Since patients cannot change position from the reference position for the radiation treatment, couplant pads are particularly helpful for ultrasound-guided radiation therapy when the target is near the skin or under an irregular surface. Thus, couplant pads are extremely useful for determining replanning times in adaptive radiotherapy.

5. Conclusion

In this study, a patient-specific 3D couplant pad (CP) was developed that has a proper acoustic property as a couplant material. Improved contrast of the US image was achieved due to using CP. The CP was easy to make with the low cost and it took a short time to make. The inherent depth of the CP provides an additional benefit of removing dead-zone artifacts. The flat surface of the CP faced to the US probe can potentially reduce the scanning time removing the dependence on sweeping direction and multi-path artifact. The patient-specific shape of the CP can remove irregular surfaces of a patient thus improving detectability of the US probe tracked by an optical camera system. The higher image contrast enabled by the use of CP can improve the efficiency and accuracy in target delineation especially for superficial target. Inter-user variation in US sanning can also be mitigated by using the CP.

Ultrasound technology can be more facilitated in radiation therapy by the developed couplant pad in addition to its conventional advantage of non-invasiveness. It is also applicable daily to the patient without any considerations for the target position. Instead of the use of x-ray, the US with using this couplant pad is more effective in IGRT in order to determine the re-treatment planning time point than the conventional x-ray imaging.

References

1. Cho KH. The challenges faced by the korean society for radiation oncology in the national healthcare system in korea. *Int J Radiat Oncol Biol Phys* 2014;90:725-728.
2. Fontanarosa D, van der Meer S, Bamber J, et al. Review of ultrasound image guidance in external beam radiotherapy: I. Treatment planning and inter-fraction motion management. *Phys Med Biol* 2015;60:R77-114.
3. Lattanzi J, McNeeley S, Pinover W, et al. A comparison of daily ct localization to a daily ultrasound-based system in prostate cancer. *Int J Radiat Oncol Biol Phys* 1999;43:719-725.
4. Langen KM, Pouliot J, Anezinos C, et al. Evaluation of ultrasound-based prostate localization for image-guided radiotherapy. *Int J Radiat Oncol Biol Phys* 2003;57:635-644.
5. Van den Heuvel F, Powell T, Seppi E, et al. Independent verification of ultrasound based image-guided radiation treatment, using electronic portal imaging and implanted gold markers. *Med Phys* 2003;30:2878-2887.
6. C. Enke KA, C.B. Saw, W. Zhen, R.B. Thompson, N.V. Raman. Inter-observer variation in prostate localization utilizing bat. *Int J Radiat Oncol Biol Phys* 2002;54:Supplement, pages 269.
7. Fiandra C, Guarneri A, Munoz F, et al. Impact of the observers' experience on daily prostate localization accuracy in ultrasound-based igrt with the clarity platform. *J Appl Clin Med Phys* 2014;15:4795.

8. Fuss M, Cavanaugh SX, Fuss C, et al. Daily stereotactic ultrasound prostate targeting: Inter-user variability. *Technol Cancer Res Treat* 2003;2:161-170.

9. Serago CF, Chungbin SJ, Buskirk SJ, et al. Initial experience with ultrasound localization for positioning prostate cancer patients for external beam radiotherapy. *Int J Radiat Oncol Biol Phys* 2002;53:1130-1138.

10. Molloy JA, Chan G, Markovic A, et al. Quality assurance of u.S.-guided external beam radiotherapy for prostate cancer: Report of aapm task group 154. *Med Phys* 2011;38:857-871.

11. http://www.bats.ac.nz/resources/physics.php

12. Acr practice parameter for the performance of a breast ultrasound examination, amended 2014 (resolution 39). ACR (American College of Radiology).

13. Goodsitt MM, Carson PL, Witt S, et al. Real-time b-mode ultrasound quality control test procedures. Report of aapm ultrasound task group no. 1. *Med Phys* 1998;25:1385-1406.

14. Burlew MM, Madsen EL, Zagzebski JA, et al. A new ultrasound tissue-equivalent material. *Radiology* 1980;134:517-520.

15. Madsen EL, Frank GR Dong F. Liquid or solid ultrasonically tissue-mimicking materials with very low scatter. *Ultrasound Med Biol* 1998;24:535-542.

16. Bush NL Hill CR. Gelatine-alginate complex gel: A new acoustically tissue-equivalent material. *Ultrasound Med Biol* 1983;9:479-484.

17. Browne JE, Ramnarine KV, Watson AJ, et al. Assessment of the acoustic properties of common tissue-mimicking test phantoms. *Ultrasound Med*

Biol 2003;29:1053-1060.

18. Zell K, Sperl JI, Vogel MW, et al. Acoustical properties of selected tissue phantom materials for ultrasound imaging. *Phys Med Biol* 2007;52:N475-484.
19. Klucinec B. The effectiveness of the aquaflex gel pad in the transmission of acoustic energy. *J Athl Train* 1996;31:313-317.
20. Tsui BCH Tsui J. A flexible gel pad as an effective medium for scanning irregular surface anatomy. *Can J Anesth* 2011;59:226-227.
21. Yasukawa K, Kunisue T, Tsuta K, et al. P6c-9 an ultrasound phantom with long-term stability using a new biomimic soft gel material. Ultrasonics Symposium, 2007. IEEE. 20072501-2502.
22. Biller DS Myer W. Ultrasound scanning of superficial structures using an ultrasound standoff pad. *Veterinary Radiology* 1988;29:138-142.
23. Culjat MO, Goldenberg D, Tewari P, et al. A review of tissue substitutes for ultrasound imaging. *Ultrasound Med Biol* 2010;36:861-873.
24. Fedorov A, Beichel R, Kalpathy-Cramer J, et al. 3d slicer as an image computing platform for the quantitative imaging network. *Magn Reson Imaging* 2012;30:1323-1341.
25. Pinter C, Lasso A, Wang A, et al. Slicerrt: Radiation therapy research toolkit for 3d slicer. *Med Phys* 2012;39:6332-6338.
26. Deasy JO, Blanco AI Clark VH. Cerr: A computational environment for radiotherapy research. *Med Phys* 2003;30:979-985.
27. Fleiss JL. Statistical methods for rates and proportions. 2nd ed. New York: John Wiley.
28. Landis JR Koch GG. The measurement of observer agreement for

categorical data. *Biometrics* 1977;33:159-174.

29. Kuban DA, Dong L, Cheung R, et al. Ultrasound-based localization. *Seminars in Radiation Oncology* 2005;15:180-191.

30. Janelle AM, Shiv S Bernard FS. A method to compare supra-pubic ultrasound and ct images of the prostate: Technique and early clinical results. *Medical Physics* 2004;31:433.

31. Hoffelt SC, Marshall LM, Garzotto M, et al. A comparison of ct scan to transrectal ultrasound-measured prostate volume in untreated prostate cancer. *Int J Radiat Oncol Biol Phys* 2003;57:29-32.

32. Narayana V, Roberson PL, Pu AT, et al. Impact of differences in ultrasound and computed tomography volumes on treatment planning of permanent prostate implants. *Int J Radiat Oncol Biol Phys* 1997;37:1181-1185.

33. Bude RO Adler RS. An easily made, low-cost, tissue-like ultrasound phantom material. *J Clin Ultrasound* 1995;23:271-273.

34. Abu-Zidan FM, Hefny AF Corr P. Clinical ultrasound physics. *J Emerg Trauma Shock* 2011;4:501-503.

35. Cosby KS Kendall JL. Practical guide to emergency ultrasound: Lippincott Williams & Wilkins; 2006.

36. Mohler ER. Essentials of vascular laboratory diagnosis. Hoboken: Hoboken : Wiley, 2008.; 2008.

37. Robinson D, Liu D, Steciw S, et al. An evaluation of the clarity 3d ultrasound system for prostate localization. *J Appl Clin Med Phys* 2012;13:100-112.

38. Lachaine M Falco T. Intrafractional prostate motion management with the clarity autoscan system. *Med Phys Int.* 2013;1:72-80.

39. Fargier-Voiron M, Presles B, Pommier P, et al. Impact of probe pressure variability on prostate localization for ultrasound-based image-guided radiotherapy. *Radiother Oncol* 2014;111:132-137.

40. Claes HP, Reygaerts DO, Boven FA, et al. An echo-free silicone elastomer block for ultrasonography. *Radiology* 1984;150:596.

41. Yeh HC Wolf BS. A simple portable water bath for superficial ultrasonography. *Am J Roentgenol* 1978;130:275-278.

Abstract (in Korean)

국 문 초 록

현재까지 영상유도방사선치료에 사용되는 있는 초음파 시스템은 초음파용 젤을 이용하여 행해지고 있다. 하지만 경사가 심한 표면이나 불규칙한 굴곡을 갖는 표면을 스캔하다 보면 마커 검출이 불가능해진다. 또한 이미 알려진 바 대로, 초음파는 사용자에 따라 측정 오차가 발생할 수 있으며 프로브에 가해지는 압력에 크게 영향을 받는다. 그리고 피부와 가까운 치료병변은 dead zone에 의해 피부 근처의 영상왜곡이 발생한다. 따라서 본 연구는 이러한 문제점들을 개선하여 더 많은 환자에게 초음파영상유도방사선치료를 적용할 수 있도록 3D 프린팅 기술을 이용하여 환자 모형을 만들어 환자 맞춤형 couplant pad를 개발하고 이를 환자에 적용하여 임상적 유용성에 대하여 연구하였다.

단일 물질로서 물과 비슷하게 음파 감쇄가 작은 젤라틴을 기본으로 하여 couplant pad로 사용하기에 강도와 탄성이 가장 적합한 혼합 비율을 구하였다. 유방 팬텀을 제작하여 couplant pad에 의한 치료병변용 타겟에 대한 영상 대조도를 CT 영상과 비교하였다. 고의적으로 테이블 위치를 각각 다른 방향과 크기로 20번 이동시켜서 초음파시스템의 위치 정확도를 검증하였다. 총 4명의 환자에 대하여 couplant pad를 사용하였을 때와 사용하지 않았을 때 서로 다른 3명의 사용자가 초음파 스캔을 각각

수행하여 총 486장의 초음파 영상을 획득하였다. 이 중 3명의 환자에 대하여 3D 프린터로 만든 환자 피부 모형을 이용하여 젤라틴으로 3차원 couplant pad를 제작하였다. 환자 피부 윤곽은 시뮬레이션 CT 영상에서 추출하였다. 세 명의 사용자가 각각 couplant pad를 사용하였을 때와 사용하지 않았을 때 초음파 영상을 획득하였다.

초음파 시스템의 위치 정확도는 3D 벡터 크기가 couplant pad를 사용하지 않았을 경우 1.3 mm 였지만, couplant pad를 사용하였을 경우 0.9 mm로 나타났다. 첫 치료 시 US을 기준하였을 경우, couplant pad 사용에 의하여 치료 병변의 위치 오차의 3D 벡터 크기가 4.7 mm에서 3.7 mm로 감소하였고 1 SD도 2.2 mm 에서 1.7 mm 로 감소하였다. 영상 대조도 분석에서도 couplant pad를 사용하였을 때 영상대조도가 전반적으로 10% 증가하는 것을 확인하였다. 초음파 스캔 범위와 프로브에 가해지는 압력에 의한 치료병변의 모양 변형에 대한 영향을 분석한 결과, 치료병변의 위치정합 후 질량중심의 오프셋이 couplant pad를 사용함으로 인하여 4.4 mm에서 2.9 mm로 감소하였다. Kappa value를 이용한 치료병변 모양의 일치도 분석에서는 3명의 환자들에서는 couplant pad를 사용유무와 상관없이 좋은 일치도를 보였으며 1명의 환자에서는 couplant pad를 사용함으로서 0.07에서 0.31로 일치도가 크게 향상되었다.

본 연구에서 개발한 couplant pad를 초음파영상유도방사선치료에 사용하면 보다 선명한 초음파 영상획득이 가능하고 사용자나 치료병변의 위치에 상관없이 초음파 영상을 획득할 수 있어 기존보다 많은 환자에게 적용이 가능하다. 또한 매일 치료병변의 위치 및 모양 확인이 가능하기

때문에 기존의 x-ray를 이용하는 것 보다 재 치료계획 시점을 정하는데 있어서 더 효과적일 것으로 예상한다.

주요어 : 초음파, 영상유도방사선치료, 3D couplant, 환자맞춤형 패드

학 번 : 2009-31099